

Salvador Gonzalez, Virginia Sanchez,  
Susanne Lange-Asschenfeldt,  
and Martina Ulrich

## Key Points

- Reflectance confocal microscopy (RCM) is a novel in vivo, noninvasive imaging method and real-time examination of the skin.
- It consists of a low-power, near-infrared laser light source attached to a confocal microscope, which illuminates a small skin area with a resolution comparable to conventional histology.
- It provides in vivo real-time images of the skin in a horizontal bright gray scale.

## Introduction

Reflectance confocal microscopy (RCM) is a novel in vivo, noninvasive imaging method that has already demonstrated to be highly useful in diagnosis approach and therapeutic monitoring of skin cancer [1–3]. Validation of RCM for the diagnosis and prognosis of skin tumors, including melanocytic lesions, has been extensively correlated with dermoscopy and conventional histology [4, 5]. This technology is based on a low-power, near-infrared laser light source attached to a confocal microscope, which illuminates a small skin area. Backscattered light is sent through a pinhole, which only permits in-focus plane (confocal) light to reach the point detector and eliminates the light coming from out-of-focus planes. This results in a real-time transversal thin section image of the skin (XY-axis) with a resolution comparable to conventional histology (1  $\mu\text{m}$  lateral and 3  $\mu\text{m}$  of section thickness). Upward and downward movements of the lens change the depth of the confocal plane and permit the collection of sequential planes of the studied skin sample (Z-axis). Until now the maximum depth of cutaneous study obtained with this technology is 250  $\mu\text{m}$  below the skin surface [6]. Light reflection depends on the refractive index of the different elements of the tissue, which is higher when the size of the illuminated structure is similar to the laser wavelength. At present, the most typical light utilized for RCM is a low-power (<20 mW) diode laser with 830 nm that maximizes reflection and

---

S. Gonzalez (✉)  
Dermatology Service,  
Ramon y Cajal Hospital, Alcalá University,  
Madrid, Spain

Dermatology Service,  
Memorial Sloan-Kettering Cancer Center,  
New York, NY, USA  
e-mail: gonzals6@mskcc.org

V. Sanchez  
Dermatology Service,  
CEU University,  
Madrid, Spain

S. Lange-Asschenfeldt • M. Ulrich  
Department of Dermatology,  
Charité – Universitätsmedizin,  
Berlin, Germany

prevents tissue damage. Consequently, confocal images are observed in a bright gray scale based on “endogenous contrasts” which are higher for structures containing melanin and keratin. Unlike traditional histology, RCM provides *in vivo*, real-time, in a bright gray scale horizontal images of the skin. The major disadvantages of confocal microscopy are the limited depth of imaging and the lack of exogenous contrast agents, even though current investigations are attempting to overcome these problems.

---

## Normal Skin

Before using RCM for the diagnosis of skin tumors or other noncancer skin diseases, it is necessary to describe confocal imaging of normal skin. There are different factors that affect the real-time, *in vivo* visualization of the skin by confocal microscopy, mainly the area of study, the age, and the Fitzpatrick’s phototype. Generally, confocal study starts in the outermost layer and progresses in depth. Stratum corneum appears as a variable refractive surface separated by dark linear valleys (dermatoglyphs) (Fig. 17.1a), which vary in depth depending on the skin area, the phototype of the patient, and the accumulated sun exposure. Corneocytes are observed as 25–50  $\mu\text{m}$  in size, bright, polygonal, flattened, and anucleated cells. Granular and spinous layers are constituted by cells with dark central oval-shaped nuclei and bright cytoplasm. The borders of these keratinocytes are well demarcated and constitute a “honeycombed pattern” (Fig. 17.1b). Basal layer appears as one layer of small cuboid nucleated cells which are usually more brilliant due to the high content in melanin. Consequently, confocal image at the basal layer in dark phototypes is usually observed as a “cobblestone pattern” (Fig. 17.1c). Dermoepidermal junction is located at 60–120  $\mu\text{m}$  in depth, and it appears as bright circular structures (“dermal papillary rings”) made of basal cells that surround certain darker areas, which correspond to the dermal papillae (Fig. 17.1d). Within these dark spaces, we may observe refractive collagen bundles and blood vessels with

inside rolling movement of erythrocytes and leukocytes.

---

## Skin Cancer

Since RCM was first used to image live human skin in 1995 [7], numerous scientific studies have been carried out mainly focusing in keratinocytic and more recently in melanocytic and other skin tumors.

---

## Malignant Keratinocytic Tumors

### Basal Cell Carcinoma (BCC)

Maybe due to the reason that basal cell carcinoma (BCC) constitutes the most frequent malignancy of the skin, this is the cutaneous condition that has been more extensively analyzed by RCM [8, 9]. General confocal features of BCC include dense structures formed by homogeneous tumor cells that present elongated monomorphic nuclei along the same axis of orientation (“nuclear polarization”) (Fig. 17.2b), which is often reflected as peripheral palisading when surrounding a tumor island in a perpendicular manner to the border (Fig. 17.2a, d). Frequently, a dark area, which is probably constituted by mucin depots surrounding the relatively refractive tumor aggregates, correlates with the “clefing” observed in traditional histology. Ulrich et al. reported 13 cases of nodular, nodulocystic, and superficial BCCs and found a good linear correlation between dark areas on RCM and thickness of peritumoral mucin [10]. Occasionally, the stroma reflectance is higher than the tumor islands, which are observed and consequently termed “dark silhouettes” (Fig. 17.2c). Also important are the frequently observed disarranged keratinocytes located above the tumor, probably caused by the chronic actinic damage that is usually associated to this type of tumor. The superficial dermal blood vessels are also affected, appearing numerous, dilated with the presence of intense leukocyte trafficking inside, and sometimes accompanied by a prominent

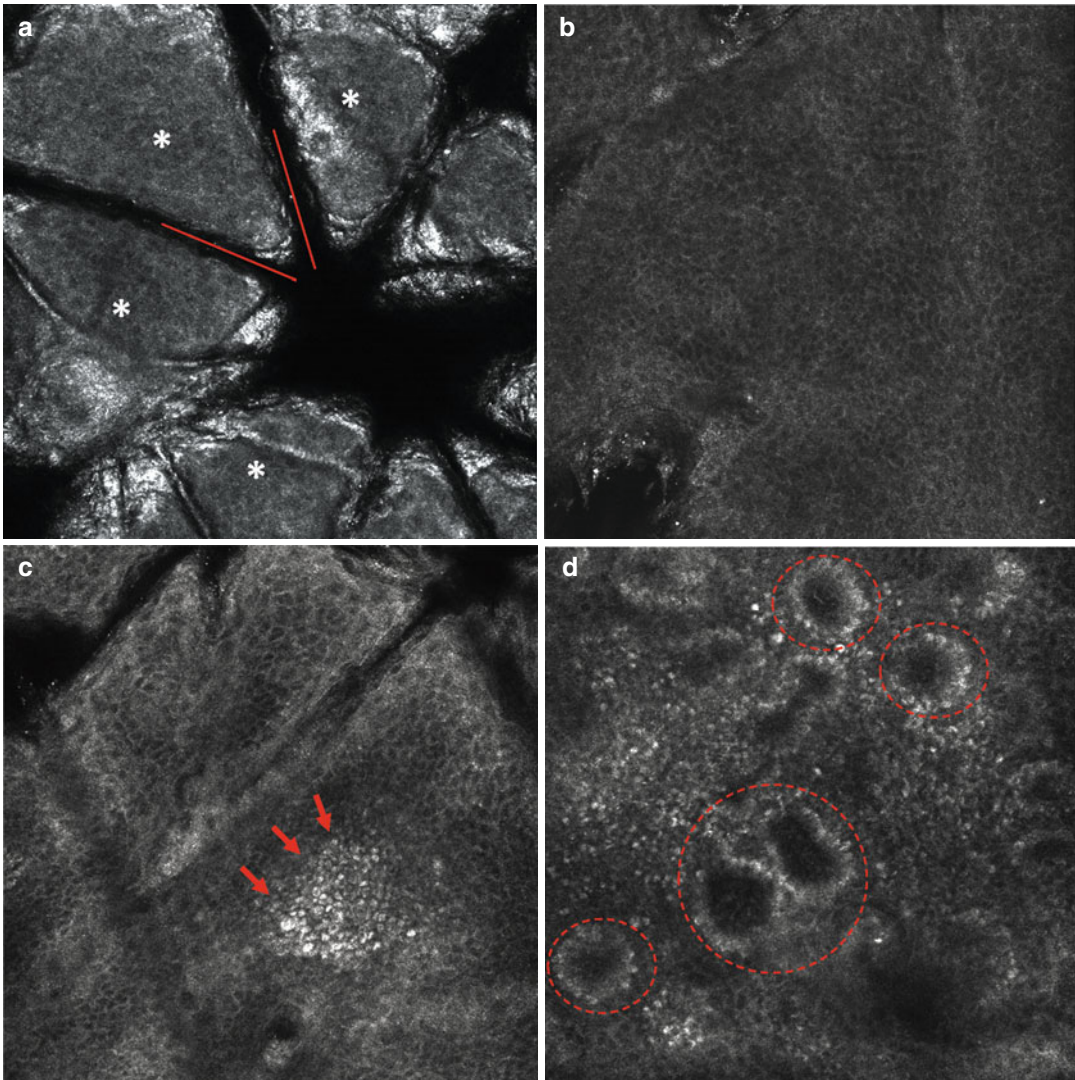


**Fig. 17.1** Shows single RCM images ( $500 \times 500 \mu\text{m}$ ) of the different layers of normal skin. Panel (a) illustrates the morphology of the stratum corneum with the presence of a variable refractive surface (*white asterisk*) separated by dark linear valleys (*red lines*) representing skin folds, (b) shows typical honeycomb pattern of the epidermis at the spinous cell layer with regular appearance of polygonal

keratinocytes, (c) shows small bright pigmented cells appearing as typical cobblestone pattern at the suprapapillary plate (*red arrows*), and (d) illustrates RCM morphology at the dermoepidermal junction (DEJ) with the presence of bright ring-like structures of pigmented basal cells (*dashed circle*)

perivascular inflammatory infiltrate [11, 12] (Fig. 17.2c). Besides, pigmented BCC presents highly refractive dendritic and granular structures inside the tumor islands correlating to dendritic melanocytes and melanosomes, respectively (Fig. 17.2d). Melanophages located in the stroma are frequently observed as bright and big, poorly demarcated structures [13, 14].

In 2004, a multicenter study was performed in a large cohort of patients to evaluate sensitivity and specificity of RCM for in vivo diagnosis of basal cell carcinoma [8]. Five major criteria were established: elongated monomorphic basaloid nuclei, polarization of these nuclei along the same axis of orientation, prominent inflammatory infiltrate, increased dermal vasculature, and

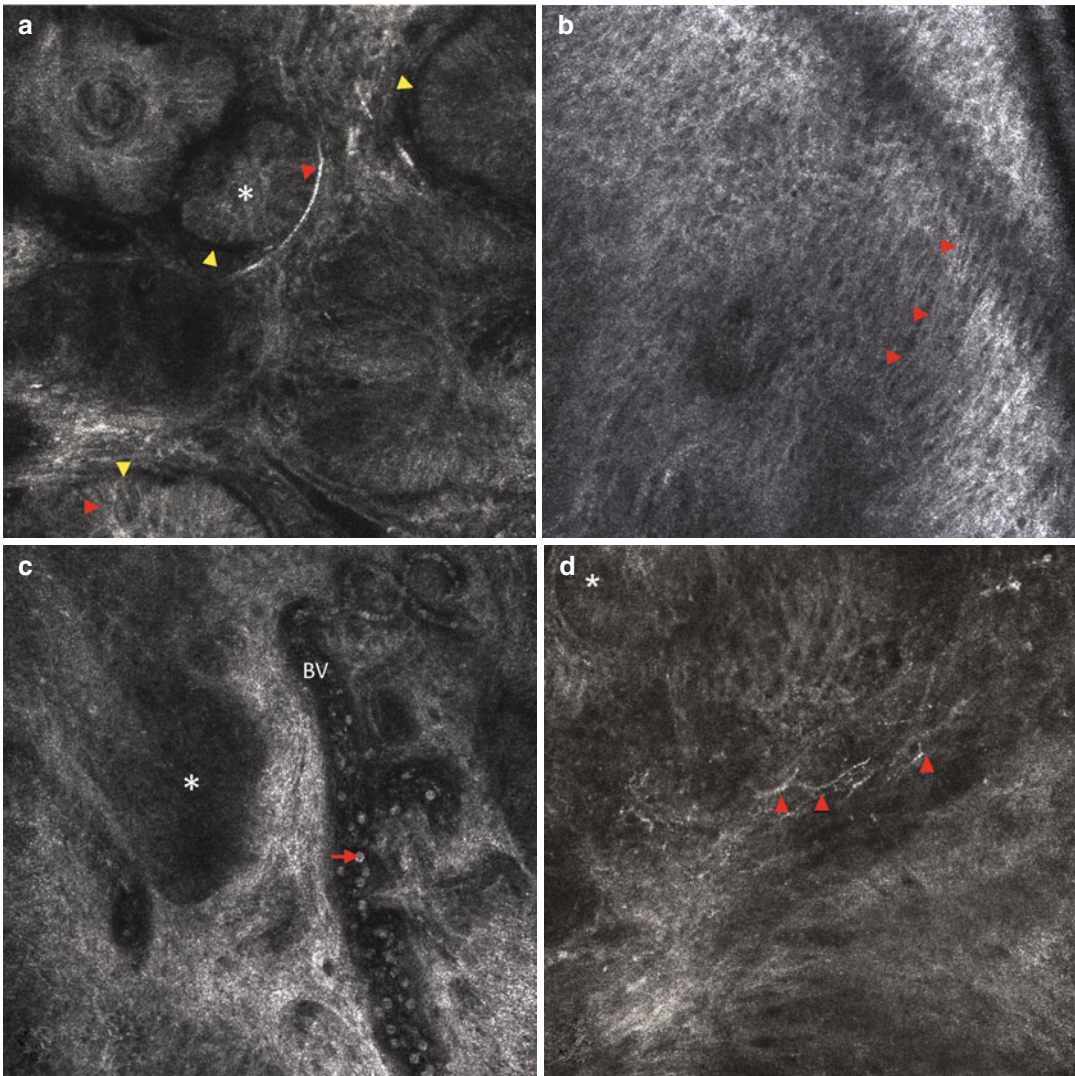


**Fig. 17.2** Basal cell carcinoma. (a) Hyporefractile tumor islands of BCC (*white asterisk*) which are separated from the surrounding stroma by dark cleft-like spaces (*yellow arrowhead*). Within the tumor islands, peripheral palisading of the cells may be observed (*red arrowhead*). (b) Nuclear streaming and elongated and polarized basal keratinocytes (*red arrowheads*). (c) Dark silhouettes (*white*

*asterisk*) and large caliber blood vessels (*BV*) with blood flow on in vivo examination. Within the *BV* single erythrocytes can be visualized (*red arrow*). (d) Tumor islands of medium refractility (*white asterisk*) surrounding by tumor stroma with collagen and inflammatory cells. Dendritic figures (*red arrowhead*) are seen

pleomorphism of the overlying epidermis. The presence of two or more criteria was found to be 100 % sensitive and 53.6 % specific for the diagnosis of BCC, while four or more RCM criteria presented 95.7 % specificity and 82.9 % of sensitivity. As expected, specificity was directly proportional to the number of criteria observed by RCM and inversely proportional to the sensitivity of the criteria in the diagnosis of BCC.

RCM has been employed in different studies that describe the main features of different histological subtypes of BCC which is important in order to determine the therapeutics and prognosis of the tumor [15]. Infiltrative BCC is visualized as ill-defined invading structures composed of very polarized cells that penetrate and deform the dermis, while nodular BCC reveals well-defined tumor islands with peripheral palisading surrounded by dark areas.

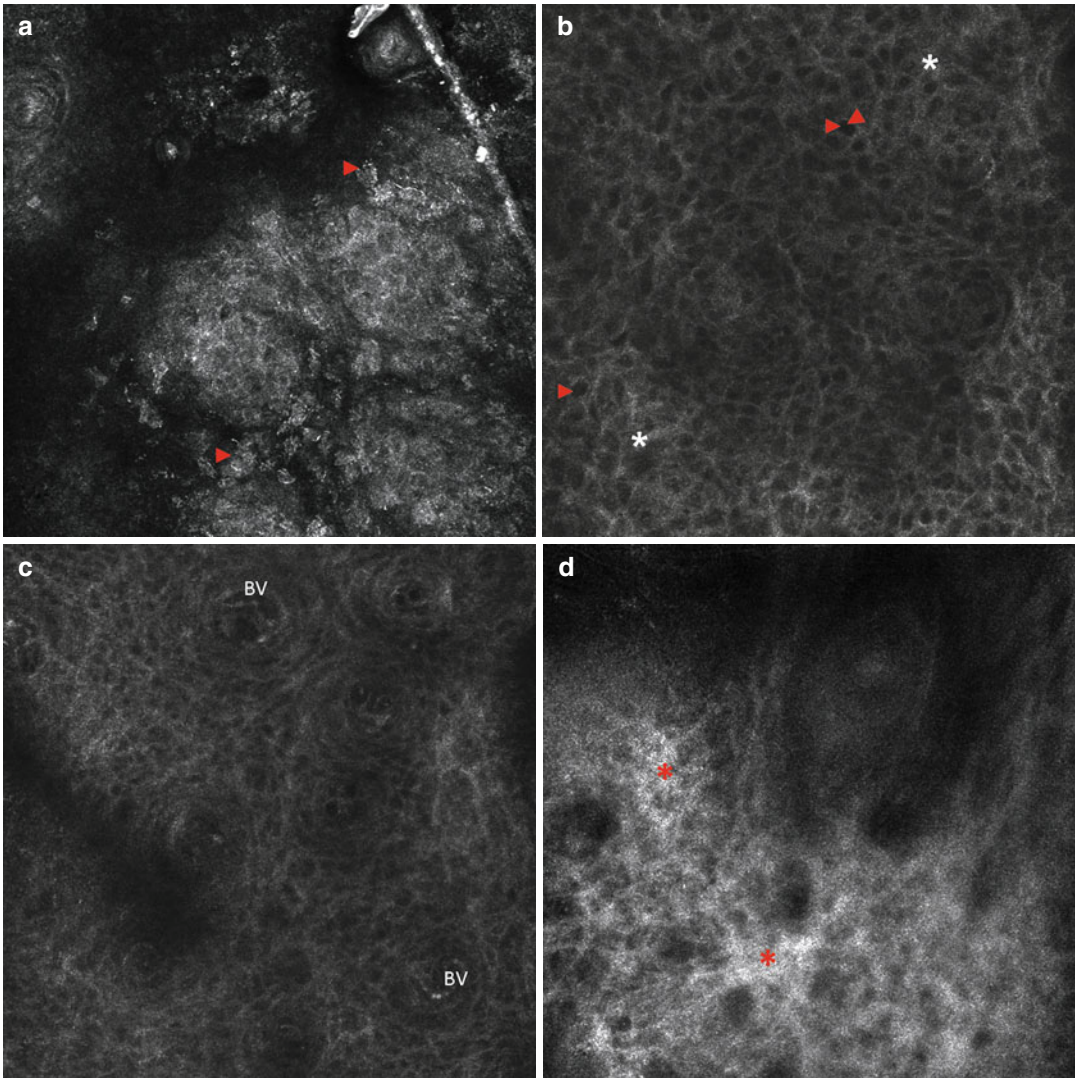


**Fig. 17.3** Representative single RCM images ( $500 \times 500 \mu\text{m}$ ) of actinic keratoses. **(a)** Disruption of the stratum corneum with single detached keratinocytes (*red arrowheads*). **(b)** Atypical honeycomb pattern of granular-spinous layers with great variation of cells and nuclei (*red arrowhead*) as

well as broadened and irregular cell borders (*white asterisk*). **(c)** Dilated blood vessels (*BV*) in the center of the dermal papillae. **(d)** Highly refractive reticulated thick fibers (*red asterisks*) which correlate to the altered collagen

## Squamous Neoplasia

Squamous neoplasia derives from epidermal keratinocytes and is among the most common cutaneous malignancies. RCM features of invasive squamous cell carcinoma (SCC) and actinic keratosis (AK) have been previously described and have good correlation with histopathology [16–18]. At the corneum layer, some amorphous, variably refractive structures can be observed

(Fig. 17.3a), which correspond to the scales of the lesion. At this level, some nucleated polygonal cells can be visualized as sharply delineated cells with a refractive thin outline surrounding a dark nucleus, corresponding to the parakeratotic cells of the histology. At the granular and spinous layers, the typical honeycombed pattern is altered and formed by pleomorphic cells with irregular size and shape (Fig. 17.3b). When there is severe atypia, the honeycombed pattern is replaced by

a completely disarranged epidermal pattern. Dyskeratotic cells in the granular and spinous layers can also be seen with confocal microscopy as sharply delineated round structures surrounding a dark oval space (nucleus). Another characteristic feature is observed inside the dermal papillary rings as round dark spaces with infrequent leukocyte trafficking inside (Fig. 17.3c). These spaces correspond to the typical dotted and glomerular vessels seen in dermoscopy of SC [19]. Confocal imaging of the upper dermal layer generally reveals extensive highly refractive reticulated thick fibers which correlates to the altered collagen that constitutes the solar elastosis commonly found in this malignancy (Fig. 17.3d). An increasing number and frequency of all these abnormal RCM features can be visualized along the spectrum of squamous neoplasia. A recent study by Ulrich et al. evaluated ten cases of Bowen's disease (BD) by RCM and correlated the findings to routine histology [20]. The most prevalent features were stratum corneum disruption, atypical honeycomb pattern, presence of two types of targetoid cells, and round-to-oval dermal blood vessels. They also observed parakeratosis, inflammatory infiltrate, and multinucleated cells. The results of this study show that RCM can be used for rapid in vivo diagnosis of BD and its distinction from other non-melanocytic skin cancer and inflammatory simulators like psoriasis or eczema.

The detection of dermal RCM features of AK, BD, and SCC may be limited by the presence of significant hyperkeratosis which sometimes worsens its optical resolution in deeper areas. To solve this problem, some chemical or physical methods can be previously applied to remove the scales.

## Melanoma

Melanoma is a malignant proliferation of melanocytes in which prognosis is related to depth of dermal invasion. This skin cancer is curable if diagnosed and excised at early stages which explains the importance of an early diagnosis [21]. Clinical diagnosis of melanoma is based on

the ABCD criteria, but the accuracy of this method is as low as 64 % [22]. To avoid unnecessary surgical biopsies, which are painful and time-consuming and leave scars, noninvasive techniques for improving clinical diagnostic accuracy are being developed such as dermoscopy, high-frequency ultrasound, optical coherence tomography, magnetic resonance imaging, and RCM [6]. For its ability to explore at cellular level resolution skin structures up to 200  $\mu\text{m}$  in depth, horizontal imaging, and noninvasiveness, RCM may be understood as a natural link between dermoscopy and histopathology, especially useful for diagnosis of early melanomas.

In the recent years, a good correlation between confocal aspects and specific dermoscopic features, such as pigment network, peripheral streaks, or pigment globules, has been demonstrated as well as the correspondence of confocal mosaics at dermoepidermal junction and global dermoscopic patterns [23–25]. Atypical pigment network, characteristic of atypical nevi and melanoma, corresponds to “non-edged papillae,” while irregular pigment globules correspond to irregularly shaped clusters formed by atypical cells in melanomas or regular cytology in benign lesions. Pigment dots are clearly visualized by RCM as pagetoid melanocytes in melanoma that are easily distinguished from the melanin clumps typically found in common nevi [26]. Moreover, RCM is particularly useful for the interpretation of the bluish pigmentation and for differentiating the plump bright cells infiltrating the dermal papillae that correspond to melanophages from the malignant melanocytes that, singularly or in clusters, infiltrate the dermis in invasive melanomas [27, 28].

In a similar manner, the main histopathological features of melanoma have been identified with RCM showing high sensitivity and specificity values [5, 29]: altered epidermal architecture with pagetoid cells (Fig. 17.4a, b), ill-defined dermal papillae with cytological atypia at dermoepidermal junction (Fig. 17.4c), cerebriform clusters, and nucleated cells in superficial dermis (Fig. 17.4d). Furthermore, very high sensitivity and specificity values of some confocal aspects, such as melanocyte cytology, disarray of the

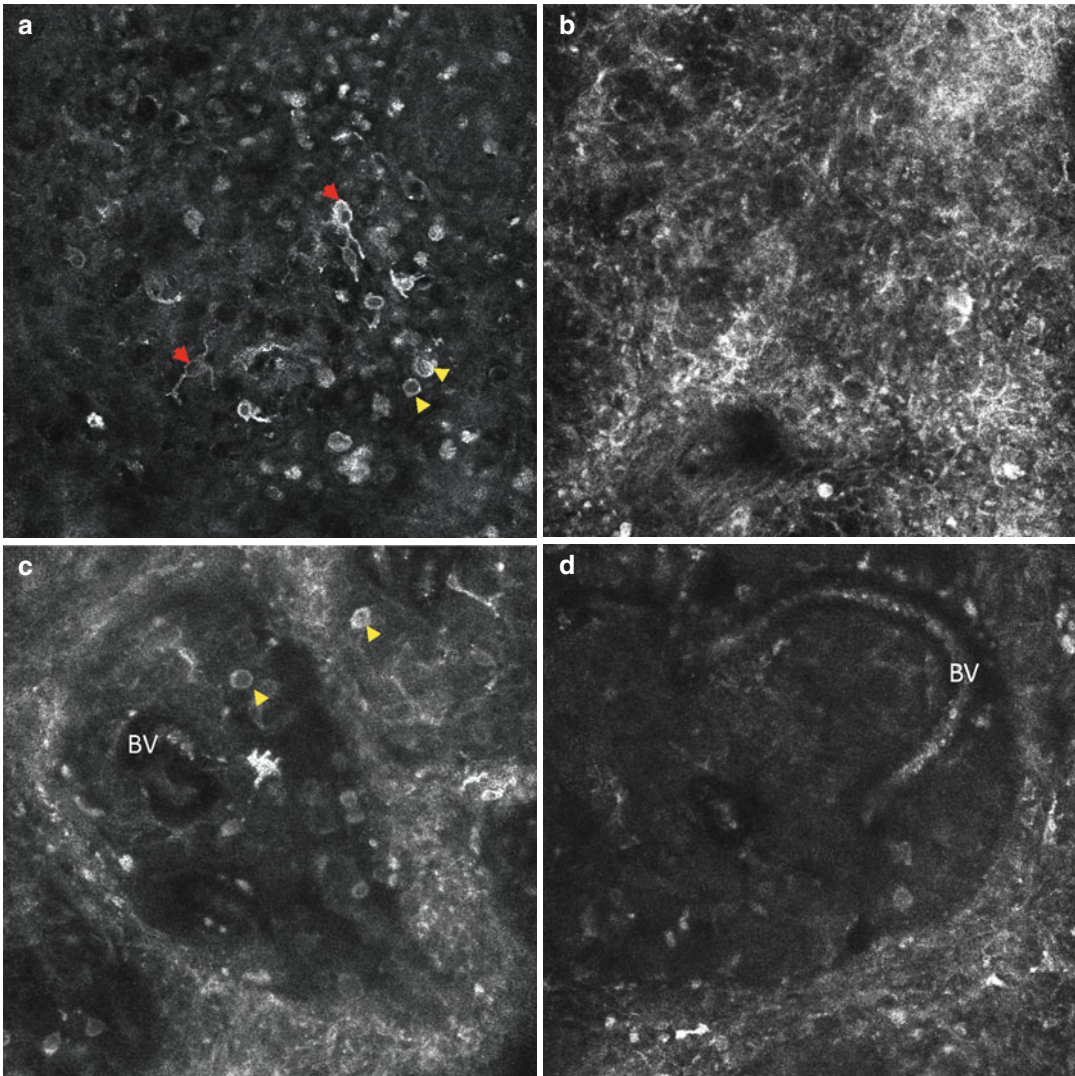


**Fig. 17.4** Representative single RCM images ( $500 \times 500 \mu\text{m}$ ) of melanoma. (a) Presence of both dendritic (*red arrowhead*) and round (*yellow arrowhead*) pagetoid melanocytes in upper epidermal layers. (b) Complete disruption of the epidermal

architecture resulting in a disarranged pattern. (c) Atypical melanocytes at the DEJ (*yellow arrowheads*) as well as in the dermal papillae containing blood vessels (BV). (d) Large dilated and elongated blood vessels (BV) in the upper dermis

architecture, and poorly defined keratinocyte cell borders, were identified by Gerger et al., comparing two preselected images per lesion from a database of 27 melanomas and 90 nevi, the majority of which corresponded to clearly benign lesions [30].

At present, two different confocal diagnosis algorithms for melanoma have been developed. Based on 102 melanocytic lesions, six criteria were identified as independently correlated with a

melanoma diagnosis, and a diagnostic algorithm was developed [31]. Two major criteria were scored 2 points, corresponding to the cytological atypia at basal cell layers and non-edged papillae at dermoepidermal junction. Four minor criteria, represented by the presence of roundish cells in superficial layers spreading upwards in a pagetoid fashion, pagetoid cells widespread throughout the lesion, cerebriform clusters in the papillary dermis, and nucleated cells within dermal papilla,

were scored 1 point. Considering a threshold score equal to or greater than 3, 97.3 % sensitivity and 72.3 % specificity were obtained, whereas increasing the threshold, specificity can be increased with a consequent decrement of sensitivity. Recently, the validity of the algorithm was blindly tested on a larger population of equivocal melanocytic lesions, showing in a reproducible clinical setting a 92 % sensitivity and 70 % specificity [5]. Segura et al. developed a two-step method for the diagnosis of melanoma by RCM [32]. In a preliminary study, they evaluated 154 skin tumors, including 100 melanocytic and 54 non-melanocytic lesions, by RCM before their excision. They observed four confocal features that differentiated melanocytic from non-melanocytic lesions: cobblestone pattern of epidermal layers, pagetoid spread, mesh appearance of the dermoepidermal junction, and the presence of dermal nests. Within melanocytic lesions, the presence of roundish suprabasal cells and atypical nucleated cells in the dermis was associated with melanoma, and the presence of edged papillae and typical basal cells was associated with nevi. Furthermore, a recent study [33] tried to determine whether specific histological features in dysplastic nevi had reliable correlates on confocal microscopy and developed an *in vivo* microscopic grading system, which consists in a simplified algorithm to distinguish dysplastic nevi from melanoma and non-dysplastic nevi. Sixty melanocytic lesions with equivocal dermatoscopic aspects were analyzed by RCM and histopathology, and they found good correlation between their features. As observed by RCM, dysplastic nevi were characterized by a ringed pattern, in association with a meshwork pattern in a large proportion of cases, along with atypical junctional cells in the center of the lesion and irregular junctional nests with short interconnections. The simultaneous presence of cytological atypia and of atypical junctional nests (irregular, with short interconnections, and/or with nonhomogeneous cellularity) was consistent with histological dysplasia, whereas widespread pagetoid infiltration, widespread cytological atypia at the junction, and non-edged papillae suggested melanoma diagnosis.

Interestingly, several confocal features for melanoma may be also identified in amelanotic

melanomas. It is possible to detect melanocytes in a clinically amelanotic tumor due to the presence of some melanin inside the pre-melanosomes, which have similar size to the wavelength that we use for imaging. Considering that amelanotic tumors do not present a high refractivity as other heavily pigmented lesions, they may be more easily diagnosed with RCM than with dermoscopy, which suggests a better early diagnosis of certain clinically difficult pigmented lesions such as amelanotic melanoma [34].

## **Mycosis Fungoides**

Mycosis fungoides (MF) represents the most common form of cutaneous T-cell lymphoma [29]. The clinical presentation may be diverse and, in the first stages, usually shows an indolent course with stable or slowly progressing lesions that may resemble chronic eczema or plaque psoriasis. Due to this reason, early diagnosis of the disease is frequently delayed. MF final diagnosis is based on histopathological evaluation in combination with immunohistochemistry and clonality studies.

In recent years, the main RCM features of MF have been published [35, 36]. RCM reveals the major features of MF such as exocytosis and Pautrier microabscesses, although early diagnosis of MF remains challenging. However, confocal microscopy may be useful to select highly suspicious lesions for biopsy and help to accelerate diagnosis.

At the patch stage of MF, the changes may be very subtle, and consequently the diagnosis at this early phase with confocal microscopy may be difficult. The most important confocal features include hyporefractivity of dermal papillary rings and small, weakly refractive round cells located in the spinous layer, which correlates to the interface changes and exocytosis process, respectively. In the plaque phase of MF, the visualization of typical confocal features of MF may be easier. Some small lightly refractive cells appear in the spinous layer correlating to epidermotropism of lymphocytes, which sometimes are grouped and located inside dark spaces within the epidermis corresponding to Pautrier microabscesses on histopathology. These



vesicle-like spaces have to be distinguished from those seen in acute eczema by the absence of parakeratosis and spongiosis and the presence of other MF characteristic confocal features. In tumor-type MF, the hyporefractive papillary rings and the infiltration of small lightly refractive cells in the epidermis are frequently visualized in confocal images, while the vesicle-like spaces are rarely detected. Inside papillary dermis, highly refractive cells of small to medium size are observed and blood vessels may show a well-circumscribed thickened wall.

### Clinical Applications Besides Diagnosis in Cutaneous Oncology

The high resolution obtained by RCM allows its utilization not only for diagnosis but also for surgery planning or evaluation of response to noninvasive therapies. The most important future applications are: guide for biopsy sample, preventing the “sampling error” so common in some situations like mycosis fungoides, malignant lentigo, or atypical nevus syndrome; tumor delimitation before excision in special areas, such as face or scalp, or ill-defined tumors such as malignant lentigo or amelanotic melanoma [3, 37–39]; monitoring the clinical response to noninvasive therapies for some keratinocytic tumors such as imiquimod cream or photodynamic therapy [40–43]; and for residual tumor detection after treatment [44].

#### Conclusion

RCM is an efficient tool for the study of the skin physiology and diseases. Its most important advantages are the noninvasiveness and the *in vivo* and real-time examination of the skin. Although it has been mostly utilized for cutaneous malignant tumors, some recent studies show its usefulness to diagnose other benign tumors and inflammatory skin diseases. Undoubtedly, confocal microscopy presents some technical and scientific limitations, which must be resolved before it becomes a tool of reference. It is necessary to improve imaging depth and, perhaps, to find contrast agents in order to recognize certain cell types

and subcellular structures. Furthermore, it is indispensable a training for dermatologists and dermatopathologists before they get used to horizontal sections of the skin and black and white colors. Although skin biopsy remains the gold standard in microscopic diagnosis, RCM offers an important approach for skin diagnosis.

### Glossary

**Cobblestone pattern** is the pattern found in basal layer keratinocytes, which appears as one layer of small cuboid nucleated cells usually more brilliant due to the high content in melanin. It is the confocal pattern usually observed at the basal layer in dark phototypes.

**Dark silhouettes** found in BCC refer to those areas where the stroma reflectance is higher than the tumor islands.

**Dermal papillary rings** is the confocal pattern found at the dermoepidermal junction and it appears as bright circular structures made of basal cells that surround certain darker areas, which correspond to the dermal papillae.

**Dermatoglyphs** dark linear valleys

**Honeycombed pattern** is the pattern found in normal keratinocytes of the granular and spinous layers. These are cells with dark central oval-shaped nuclei and bright cytoplasm.

**Nuclear polarization** refers to the elongated monomorphic nuclei along the same axis of orientation and present as a general confocal feature of BCC (Basal cell carcinoma). It often reflects as peripheral palisading.

**RCM** Reflectance confocal microscopy.

### References

1. Aghassi D, Anderson RR, González S. Confocal laser microscopic imaging of actinic keratoses *in vivo*: a preliminary report. *J Am Acad Dermatol.* 2000;43: 42–8.
2. Langley RG, Rajadhyaksha M, Dwyer PJ, Sober AJ, Flotte TJ, Anderson RR. Confocal scanning laser microscopy of benign and malignant melanocytic skin lesions *in vivo*. *J Am Acad Dermatol.* 2001;45: 365–76.

3. Busam KJ, Hester K, Charles C, et al. Detection of clinically amelanotic malignant melanoma and assessment of its margins by in vivo confocal scanning laser microscopy. *Arch Dermatol*. 2001;137:923–9.
4. Ulrich M, Stockfleth E, Roewert-Huber J, Astner S. Non invasive diagnostic tools for non-melanoma skin cancer. *Br J Dermatol*. 2007;157 Suppl 2:56–8.
5. Pellacani G, Guitera P, Longo C, Avramidis M, Seidenari S, Menzies S. The impact of in vivo reflectance confocal microscopy for the diagnostic accuracy of melanoma and equivocal melanocytic lesions. *J Invest Dermatol*. 2007;127:2759–65.
6. Rajadhyaksha M, González S, Zavislan JM, Anderson RR, Webb RH. In vivo confocal scanning laser microscopy of human skin II: advances in instrumentation and comparison with histology. *J Invest Dermatol*. 1999;113:293–303.
7. Rajadhyaksha M, Grossman M, Esterowitz D, Webb RH, Anderson RR. In vivo confocal scanning laser microscopy of human skin: melanin provides strong contrast. *J Invest Dermatol*. 1995;104:946–52.
8. Nori S, Rius-Diaz F, Cuevas J, et al. Sensitivity and specificity of reflectance mode confocal microscopy for in vivo diagnosis of basal cell carcinoma: a multicenter study. *J Am Acad Dermatol*. 2004;51:923–30.
9. González S, Tannous Z. Real-time, in vivo confocal reflectance microscopy of basal cell carcinoma. *J Am Acad Dermatol*. 2002;47:869–74.
10. Ulrich M, Roewert-Huber J, González S, Rius-Diaz F, Stockfleth E, Kanitakis J. Peritumoral clefing in basal cell carcinoma: correlation of in vivo reflectance confocal microscopy and routine histology. *J Cutan Pathol*. 2011;38:190–5.
11. González S, Sackstein R, Anderson RR, Rajadhyaksha M. Real-time evidence of in vivo leukocyte trafficking in human skin by reflectance confocal microscopy. *J Invest Dermatol*. 2001;117:384–6.
12. Ahlgrimm-Siess V, Cao T, Oliviero M, Hofmann-Wellenof R, Rabinovitz HS, Scope A. The vasculature of non-melanocytic skin tumors in reflectance confocal microscopy: vascular features of basal cell carcinoma. *Arch Dermatol*. 2010;146:353–4.
13. Agero AL, Busam KJ, Benvenuto-Andrade C, et al. Reflectance confocal microscopy of pigmented basal cell carcinoma. *J Am Acad Dermatol*. 2006;54:638–43.
14. Segura S, Puig S, Carrera C, Palou J, Malvey J. Dendritic cells in pigmented basal cell carcinoma: a relevant finding by reflectance-mode confocal microscopy. *Arch Dermatol*. 2007;143:883–6.
15. González S, Gill M, Halpern AC, editors. Reflectance confocal microscopy of cutaneous tumors: an atlas with clinical, dermoscopic and histological correlations. London: Informa Healthcare; 2008.
16. Ulrich M, Maltusch A, Rius-Diaz F, Röwert-Huber J, González S, Sterry W, et al. Clinical applicability of in vivo reflectance confocal microscopy for the diagnosis of actinic keratoses. *Dermatol Surg*. 2008;34(5):610–9.
17. Ulrich M, Krueger-Corcoran D, Roewert-Huber J, Sterry W, Stockfleth E, Astner S. Reflectance confocal microscopy for noninvasive monitoring of therapy and detection of subclinical actinic keratoses. *Dermatology*. 2010;220(1):15–24.
18. Rishpon A, Kim N, Scope A, Porges L, Oliviero MC, Braun RP, et al. Reflectance confocal microscopy criteria for squamous cell carcinomas and actinic keratoses. *Arch Dermatol*. 2009;145:766–72.
19. Zalaudek I, Giacomel J, Schmid K, Bondino S, Rosendahl C, Cavicchini S, et al. Dermatoscopy of facial actinic keratosis, intraepidermal carcinoma, and invasive squamous cell carcinoma: a progression model. *J Am Acad Dermatol*. 2012;66(4):589–97.
20. Ulrich M, Kanitakis J, González S, Lange-Asschenfeldt S, Stockfleth E, Roewert-Huber J. Evaluation of Bowen disease by in vivo reflectance confocal microscopy. *Br J Dermatol*. 2012;166(2):451–3.
21. Balch CM, Houghton AN, Sober AJ, Soong SJ, editors. Cutaneous melanoma. 3rd ed. St. Louis: Quality Medical Publishing; 1998.
22. Grin CM, Kopf AW, Welkovich B, Bart RS, Levenstein MJ. Accuracy in the clinical diagnosis of malignant melanoma. *Arch Dermatol*. 1990;126:763–6.
23. Scope A, Benvenuto-Andrade C, Agero AL, Halpern AC, González S, Marghoob AA. Correlation of dermoscopic structures of melanocytic lesions to reflectance confocal microscopy. *Arch Dermatol*. 2007;143:176–85.
24. Scope A, Gill M, Benvenuto-Andrade C, Halpern AC, González S, Marghoob AA. Correlation of dermoscopy with in vivo reflectance confocal microscopy of streaks in melanocytic lesions. *Arch Dermatol*. 2007;143:727–34.
25. Pellacani G, Longo C, Malvey J, Puig S, Carrera C, Segura S, et al. In vivo confocal microscopic and histopathologic correlations of dermoscopic features in 202 melanocytic lesions. *Arch Dermatol*. 2008;144(12):1597–608.
26. Pellacani G, Cesinaro AM, Seidenari S. Reflectance-mode confocal microscopy for the in vivo characterization of pagetoid melanocytosis in melanomas and nevi. *J Invest Dermatol*. 2005;125:532–7.
27. Pellacani G, Bassoli S, Longo C, Cesinaro AM, Seidenari S. Diving into the blue: in vivo microscopic characterization of the dermoscopic blue hue. *J Am Acad Dermatol*. 2007;57:96–104.
28. Segura S, Pellacani G, Puig S, Longo C, Bassoli S, Guitera P, et al. In vivo microscopic features of nodular melanomas: dermoscopy, confocal microscopy, and histopathologic correlates. *Arch Dermatol*. 2008;144:1311–20.
29. Willemze R, Jaffe ES, Burg G, Cerroni L, Berti E, Swerdlow SH, et al. WHO-EORTC classification for cutaneous lymphomas. *Blood*. 2005;105:3768–85.

30. Gerger A, Koller S, Kern T, Massone C, Steiger K, Richtig E, et al. Diagnostic applicability of in vivo confocal laser scanning microscopy in melanocytic skin tumors. *J Invest Dermatol.* 2005;124:493–8.
31. Pellacani G, Cesinaro AM, Seidenari S. Reflectance-mode confocal microscopy of pigmented skin lesions – improvement in melanoma diagnostic specificity. *J Am Acad Dermatol.* 2005;53:979–85.
32. Segura S, Puig S, Carrera C, Palou J, Malvehy J. Development of a two-step method for the diagnosis of melanoma by reflectance confocal microscopy. *J Am Acad Dermatol.* 2009;61:216–29.
33. Pellacani G, Farnetani F, Gonzalez S, Longo C, Cesinaro AM, Casari A, et al. In vivo confocal microscopy for detection and grading of dysplastic nevi: a pilot study. *J Am Acad Dermatol.* 2012;66(3):e109–21.
34. Guitera P, Pellacani G, Crotty KA, Scolyer RA, Li LX, Bassoli S, et al. The impact of in vivo reflectance confocal microscopy on the diagnostic accuracy of lentigo maligna and equivocal pigmented and nonpigmented macules of the face. *J Invest Dermatol.* 2010;130(8):2080–91.
35. Agero AL, Gill M, Ardigo M, Myskowski P, Halpern AC, González S. In vivo reflectance confocal microscopy of mycosis fungoides: a preliminary study. *J Am Acad Dermatol.* 2007;57:435–41.
36. Gill M, Agero AL, Ardigo M, Myskowski P, González S. Mycosis fungoides. In: González S, Gill M, Halpern AC, editors. *Reflectance confocal of cutaneous tumors.* London: Informa Healthcare; 2008. p. 183–92.
37. Mihm MC, Flotte TJ, González S. In vivo examination of lentigo maligna and malignant melanoma in situ, lentigo maligna type by near-infrared reflectance confocal microscopy: comparison of in vivo confocal images with histologic sections. *J Am Acad Dermatol.* 2002;46:260–3.
38. Curiel-Lewandrowski C, Williams CM, Swindells KJ, Tahan SR, Astner S, Frankenthaler RA, et al. Use of in vivo confocal microscopy in malignant melanoma: an aid in diagnosis and assessment of surgical and non surgical therapeutic approaches. *Arch Dermatol.* 2004;140:1127–32.
39. Chen CS, Elias M, Busam K, Rajadhyaksha M, Marghoob AA. Multimodal in vivo optical imaging, including confocal microscopy, facilitates presurgical margin mapping for clinically complex lentigo maligna melanoma. *Br J Dermatol.* 2005;153:1031–6.
40. Trehan M, Swindells K, Taylor CR, Racette AL, González S. Confocal microscopy imaging of actinic keratoses post-photodynamic therapy with 5-ALA. Paper presented at: 20th World Congress of Dermatology, Paris, 2002.
41. Goldgeier M, Fox CA, Zavislan JM, Harris D, González S. Noninvasive imaging, treatment, and microscopic confirmation of clearance of basal cell carcinoma. *Dermatol Surg.* 2003;29:205–10.
42. Torres A, Niemeyer A, Berkes B, Marra D, Schanbacher C, González S, et al. 5% imiquimod cream and reflectance-mode confocal microscopy as adjunct modalities to Mohs micrographic surgery for treatment of basal cell carcinoma. *Dermatol Surg.* 2004;30:1462–9.
43. Astner S, González S, Stockfleth E, Lademann J. Confocal microscopy: innovative diagnostic tools for monitoring of noninvasive therapy in cutaneous malignancies. *Drug Discov Today Dis Mech.* 2008;5(1):81–91.
44. Marra DE, Torres A, Schanbacher CF, González S. Detection of residual basal cell carcinoma by in vivo confocal microscopy. *Dermatol Surg.* 2005;31:538–41.